D 61519

PROTEOMICS

2'07

www.proteomics-journal.com

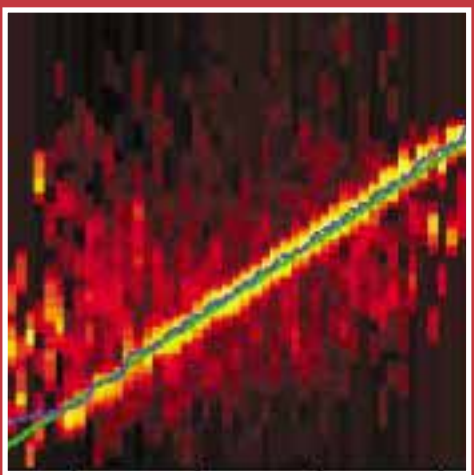

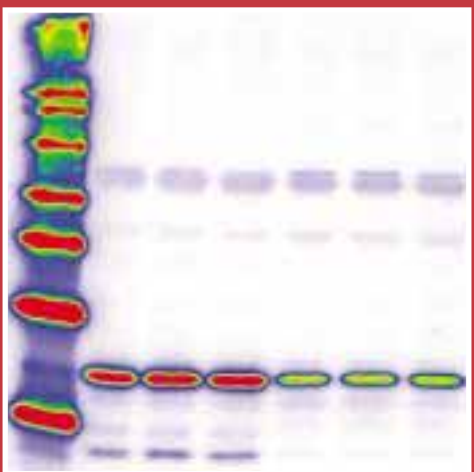

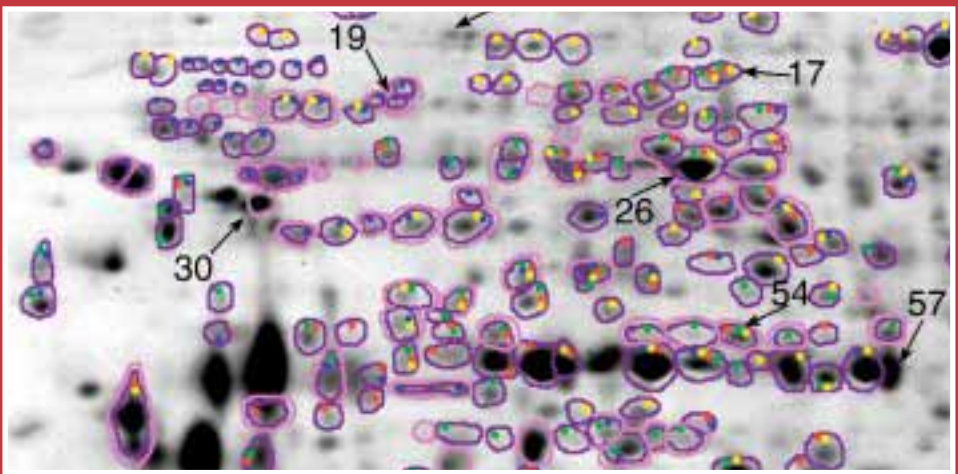

Technology
Cell Biology
Microbiology
Plant Proteomics
Animal Proteomics
Biomedicine

BICENTENNIAL 1807 WILEY 2007 BICENTENNIAL

WILEY-VCH

ISSN 1615-9853 · PROTC 7 (2) 173–330 (2007) · Vol. 7 · No. 2 · January 2007

DOI 10.1002/pmic.200600399

RESEARCH ARTICLE

A comparative proteome and phosphoproteome analysis of differentially regulated proteins during fertilization in the self-incompatible species *Solanum chacoense* Bitt.

Kateryna Vyetrogon[1], *Faiza Tebbji*[1], *Douglas J. H. Olson*[2], *Andrew R. S. Ross*[2] *and Daniel P. Matton*[1]

[1] Institut de Recherche en Biologie Végétale (IRBV), Département de sciences biologiques, Université de Montréal, Montréal, QC, Canada
[2] Plant Biotechnology Institute, National Research Council of Canada, Saskatoon, SK, Canada

Received: May 31, 2006
Revised: August 29, 2006
Accepted: October 8, 2006

We have used 2-DE for a time-course study of the changes in protein and phosphoprotein expression that occur immediately after fertilization in *Solanum chacoense*. The phosphorylation status of the detected proteins was determined with three methods: *in vivo* labeling, immunodetection, and phosphoprotein-specific staining. Using a p*I* range of 4–7, 262 phosphorylated proteins could be mapped to the 619 proteins detected by Sypro Ruby staining, representing 42% of the total proteins. Among these phosphoproteins, antibodies detected 184 proteins from which 78 were also detected with either of the other two methods (42%). Pro-Q Diamond phosphoprotein stain detected 111 proteins, of which 76 were also detected with either of the other two methods (68%). The ^{32}P *in vivo* labeling method detected 90 spots from which 78 were also detected with either of other two methods (87%). On comparing before and after fertilization profiles, 38 proteins and phosphoproteins presented a reproducible change in their accumulation profiles. Among these, 24 spots were selected and analyzed by LC-MS/MS using a hybrid quadrupole-TOF (Q-TOF) instrument. Peptide data were searched against publicly available protein and EST databases, and the putative roles of the identified proteins in early fertilization events are discussed.

Keywords:
Embryogenesis / Fertilization / Phosphoproteome / *Solanum chacoense* / Two-dimensional gel electrophoresis

Correspondence: Professor Daniel P. Matton, Institut de Recherche en Biologie Végétale (IRBV), Département de sciences biologiques, Université de Montréal, 4101 Sherbrooke Est, Montréal, QC, Canada H1X 2B2
E-mail: dp.matton@umontreal.ca
Fax: +1-514-872-9406

Abbreviations: Arm, armadillo; **HAP,** hours after pollination; **MFP1,** matrix attachment region binding filament like protein; **NAC,** nascent polypeptide associated complex; **PPi,** pyrophosphate; **ROS,** reactive oxygen species; **SEBF,** silencing element binding factor

1 Introduction

Over the last decade, numerous DNA sequencing projects have harvested a large amount of genomic and expressed sequence data. Although several high-throughput RNA expression measurement tools have been developed, with microarray analysis being at the forefront of global gene expression, these powerful techniques only look at the transcriptional regulation of a set of genes. One of the biggest hurdles in relating modulations observed at the gene expression level and their actual effects at the protein level is

the fact that mRNA levels are not always a consistent indication of a protein's abundance, and several studies have already revealed poor correlations between changes in the abundance of specific mRNAs and their corresponding proteins [1–4]. This is probably due in part to large differences in mRNA and protein stability and turnover. In addition, many proteins undergo extensive PTMs that significantly affect their activity and subcellular localization. Therefore, only the study of the proteins themselves provides information on their real amount and/or activity at a given time in a given tissue, or in response to a given stimulus or treatment [5]. Proteomic analyses also offer the opportunity to examine simultaneous changes in protein accumulation occurring in complex developmental processes, and to determine informative temporal expression patterns [6]. One of the most important developmental processes in plants is exemplified by the formation of the seed. Seed formation starts from the double fertilization process that takes place in the embryo sac of the ovule, where the two male gametes delivered by the pollen tube fertilize the two female gametes, the haploid egg cell and the diploid central cell. This event then leads to the development of the diploid embryo from the egg cell that will eventually give rise to the new sporophytic generation, and of the triploid endosperm from the central cell, an ephemeral tissue primarily involved in the nutrition of the developing embryo [7].

Although a number of proteomic studies have targeted later events during seed development, including germination [8–14], to our knowledge no proteomic or phosphoproteomic studies have yet focused on the very early stages of seed development corresponding to the period directly preceding embryo and eventually seed formation, namely the fertilization event itself. One major hurdle comes from the fact that the egg and the central cell are encased in the embryo sac, a small part only of the entire ovule, that itself is only a small part of the whole ovary. One promising approach involves the use of isolated cells, but low sensitivity due to the difficulty of harvesting the cells combined with invasive isolation methods makes this approach tedious and time-consuming, although it has been successfully used to isolate abundant proteins from the egg cell prior to fertilization [15].

Protein phosphorylation constitutes one of the most prominent type of PTM in the cell, and it mobilizes a large number of genes, especially in plants, where it contributes significantly to the complexity of the proteome [16]. It is estimated that in humans one third of all the proteins are simultaneously phosphorylated at any given time, mobilizing two percent of the genes (approximately 500 protein kinases and 100 protein phosphatases) [17, 18]. In plants, these proportions are even higher. In *Arabidopsis*, there are approximately 1100 protein kinases and between 100 and 200 protein phosphatases, which constitutes 5% of its genome [19, 20]. Classically, detection of phosphoproteins within a protein mixture relied on the combination of electrophoretic procedures to isolate proteins and either autoradiography (in the case of prior cell labeling with ^{32}P) or immunodetection using antibodies raised against phosphorylated residues [16]. Recently, an alternative approach of direct staining of gels with a phosphoprotein specific fluorophore (Pro-Q Diamond dye) was proposed [21–23].

We have recently shown through an EST sequencing project from fertilized ovules and from the fine expression analysis of the isolated plant protein receptor kinases (PRK) that most of the PRKs were modulated at the transcriptional level following pollination or fertilization [24]. In the present study, and using a similar approach, the ovary proteome and phosphoproteome during ovule fertilization will be investigated in the self-incompatible species *Solanum chacoense*, a close relative of potato and tomato. Three phosphoprotein detection methods to identify phosphoproteins differentially regulated during fertilization have been compared, and the biological relevance of the isolated proteins is discussed.

2. Materials and methods

2.1 Plant material and sampling procedure

All plant material was collected from *S. chacoense* Bitt. genotype G4 (self-incompatibility alleles $S_{12}S_{14}$). For fertilization-related events, *S. chacoense* genotype V22 (self-incompatibility alleles $S_{11}S_{13}$) was used as the pollen donor. These genotypes were obtained from crosses between line PI 458314 (self-incompatibility alleles $S_{11}S_{12}$) and line PI 230582 (self-incompatibility alleles $S_{13}S_{14}$), originally obtained from the Potato Introduction Station (Sturgeon Bay, WI, USA). In order to collect all plant material on the same day for processing and analyses, flowers were pollinated on two consecutive days: the 42 and 48 h after pollination samples on the first day, and the 30 and 36 h after pollination samples on the second day. For each sample 30 flowers were pollinated and these experiments were done in triplicate (biological triplicates) to avoid differences due to growth conditions. Flowers were immediately hand-dissected after collection and the ovaries were kept at −80°C until protein extraction.

2.2 *In vivo* labeling of the ovaries

For *in vivo* labeling, flowers were hand-pollinated in the greenhouse and 6 h, before ovary collection time, inflorescence stems bearing approximately 8–10 flowers were placed in a microtube containing 0.4 mCi of a ^{32}P-orthophosphate solution diluted in 40 μL of water (H_3PO_4, Perkin Elmer, Boston, MA, USA) for 20 min until total absorption (see Fig. 1). Immediately following the absorption, the inflorescence stems were placed in sterile water for 6 h. Absorption of ^{32}P-orthophosphate by different tissues was monitored by scintillation counting over time and after 6 h, when the ^{32}P labeling had reached the flowers, flowers were collected, dissected, and isolated ovaries were frozen at −80°C until analysis.

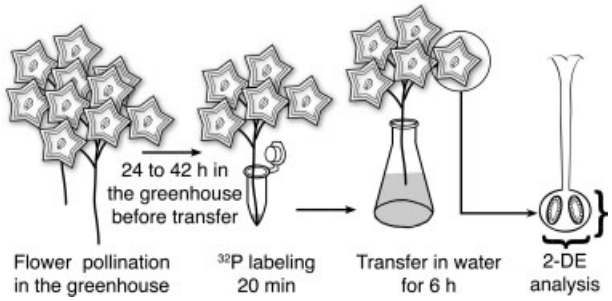

Figure 1. Schematic drawing of the method used to radioactively label ovary proteins with ^{32}P *in vivo*. After manual pollination, inflorescence stems bearing 8–10 flowers were cut and placed in a microtube containing ^{32}P-orthophosphate until total absorption. Immediately following absorption, the inflorescence stems were placed in sterile water for 6 h. Absorption of ^{32}P-orthophosphate was monitored by scintillation counting over time and 6 h was determined as optimal to get sufficient ^{32}P labeling in the ovary. Flowers were then collected, dissected, and ovaries were isolated and prepared for 2-D gel analyses.

2.3 Protein extraction

Fresh or frozen ovaries were ground in a mortar in the presence of liquid nitrogen. One hundred mg corresponding to 60 ovaries were resuspended in 1 mL of ice-cold 10% TCA/acetone, 0.07% β-mercapthoethanol and allowed to precipitate overnight at −20°C. Following precipitation, the samples were centrifuged at 14 000 rpm in a microtube centrifuge at 4°C and the precipitate was washed twice with 1 mL of cold 80% acetone and 0.07% β-mercapthoethanol. The samples were then dried by vacuum centrifugation for 1–2 min and resuspended in 300 μL of IEF sample buffer (8 M Urea, 50 mM DTT, 4% w/v CHAPS, 0.2% v/v Carrier ampholytes pH 3–10, 0.0002% w/v Bromophenol Blue) for 1 h with vigorous vortexing. Insoluble material was removed by centrifugation at 14 000 rpm in a table centrifuge for 30 min.

The protein content of the supernatant was quantified using the Bio-Rad assay (Hercules, CA, USA) based upon a modified procedure of Bradford [25] using BSA as a standard. Sixty micrograms of extracted proteins were used for gels stained with Pro-Q Diamond, while 100 μg of proteins were used for *in vivo* ^{32}P-orthophosphate labeling and 250 μg of proteins were used for antibody detection or Coomassie staining.

2.4 Second dimension electrophoresis

Proteins were resuspended in 125 μL of sample and IEF buffer with 1 nM of calyculin A phosphatase inhibitor (Calbiochem, La Jolla, CA, USA) and used to rehydrate IPG strips (Bio-Rad). For the dephosphorylation assay, calyculin A was omitted and 10 μL (1 U/μL) of alkaline phosphatase (Roche Diagnostics, Laval, QC, Canada) were added to the sample 1 h prior to rehydration. Rehydration was performed overnight at room temperature with strips covered with mineral oil. Following rehydration, the strips were blotted against absorbing paper to remove excess liquid and mineral oil, placed in the IEF tray containing the wet wicks on the electrodes, covered with new mineral oil, and focused in the Protean® IEF focusing chamber (Bio-Rad). The protocol used for focusing included three steps: (i) 15 min at 250 V with rapid slope setting, (ii) 2 h at 8000 V with rapid slope setting, (iii) 8000 V until 20 000 Vh is reached.

Following IEF, IPG strips were frozen at −20°C until the next day. After thawing (10 min), the IPG strips were removed from the focusing tray, blotted to remove excess oil, and incubated for 10 min in SDS equilibration buffer (6 M Urea, 2% w/v SDS, 0.05 M Tris/HCl pH 8.8, 20% v/v Glycerol) with 2% w/v DTT, followed with another 10 min incubation in SDS equilibration buffer containing 2.5% w/v iodoacetamide. The IPG strips were then rinsed with SDS running buffer (25 mM Tris base, 192 mM Glycine, 0.1% w/v SDS) and placed on 10% acrylamide gels. Strips were overlaid with 0.5% w/v agarose in SDS running buffer with a trace of Bromophenol Blue. Second-dimension SDS-PAGE was performed in the Mini-PROTEAN® Dodeca cell (Bio-Rad) at 200 V for 45 min and at 4°C or until the Bromophenol blue dye started migrating off the gel. Following migration, the gels were either subjected to Western blotting or stained with a specific protein stain.

2.5 Gel staining

For Pro-Q Diamond Phosphoprotein staining (Molecular Probes, Eugene, OR, USA), the gels were fixed overnight in the Pro-Q Diamond Fix solution (50% v/v methanol, 10% v/v acetic acid) at room temperature with gentle agitation. On the next day, the gels were incubated in fresh Pro-Q Diamond Fix solution for 30 min. The gels were then washed three times for 10 min with water and stained with the Pro-Q Diamond Phosphoprotein stain for 47 min. Longer staining periods increased the total number of proteins detected but significantly decreased the specificity of the phosphoprotein dye. The gels were then immediately destained in the destaining solution (20% v/v 1,2-propanediol, 50 mM sodium acetate, pH 4.0) for 1 h followed by a second destain step for 1 h. The gels were then rinsed with water and scanned with a Typhoon 9200 phosphorimager (GE Healthcare, Baie d'Urfé, QC, Canada) using 532 nm excitation and the 610 BP 30 emission filter. Following the scan, the gels were then stained with Sypro Ruby (Molecular Probes, Eugene, OR, USA) overnight at room temperature with gentle agitation. The gels were then washed with 10% v/v methanol, 7% v/v acetic acid for 30 min at room temperature with gentle agitation. The gels were finally rinsed with ultrapure distilled water and scanned using 582 nm excitation and the 610 BP 30 emission filter.

Gels that contained ^{32}P-labeled proteins were stained with Sypro Ruby only, dried for 3 h in a GelAir Dryer (Bio-Rad), and scanned using 582 nm excitation and the 610 BP 30 emission filter with a Typhoon 9200 phosphorimager for

total protein pattern. The dried gels were then exposed with one intensifying screen on Kodak Biomax MR film (Interscience, Markham, ON, Canada) for up to 2 weeks at room temperature.

For CBB staining, the gels were stained overnight with 0.25% w/v CBB G-250, 10% v/v methanol, 10% v/v acetic acid, and then washed several times for 30 min with 10% v/v methanol, 10% v/v acetic acid until complete background destaining.

2.6 Western blotting and immunodetection

After 2-DE, the proteins were transferred electrophoretically onto PVDF membranes in 25 mM Tris base, 192 mM glycine, and 20% v/v methanol. After transfer, the membranes were stained with Ponceau Red and then scanned with a digital scanner (AGFA Duoscan T1200, Toronto, ON, Canada). The membranes were then washed with 25 mL TBS (20 mM Tris-HCl, 150 mM NaCl, pH 7.6) and blocked for 1 h with 25 mL of blocking buffer (TBS with 0.1% v/v Tween-20 and 5% w/v BSA) at room temperature with gentle agitation. Following blocking, the membranes were washed three times for 5 min each with 15 mL of TBS wash buffer (TBS with 0.1% v/v Tween-20) and then incubated with the primary antibody (a mix of mAb from either the Phosphoserine, Phosphothreonine, or Phosphotyrosine Detection Kits, Calbiochem) diluted in blocking buffer at a concentration of 1 μg/mL overnight at 4°C with gentle agitation. Following the incubation, the membranes were washed three times for 5 min each with 15 mL of TBS wash buffer and then incubated with the secondary antibody (fluorescein-conjugated goat antimouse total IgG, Calbiochem) diluted in blocking buffer at a concentration of 1 μg/mL for 1 h at room temperature with gentle agitation. Following the incubation, the membranes were washed again three times for 5 min each with 15 mL of TBS wash buffer and then scanned using Typhoon 9200 phosphorimager using 532-nm excitation and the 526 SP emission filter.

2.7 Image analysis

Image analysis of the gels stained with Pro-Q Diamond and Sypro Ruby was carried out with the Image Master 2D Elite software (GE Healthcare). Spots were detected with a peak dilation method. The parameters used were: background intensity 13, step size 14, smoothing size 12, minimum width-to-height ratio 0.2, and maximum width-to-height ratio 10. Other parameters managed by the software were used at their default settings. Some manual corrections were performed in order to ensure the same spots were detected between different gels. For background subtraction, the nonspot method was used. For normalization, the total volume multiplied by total area method was used. After spot detection on all gels, triplicates of the same gel were combined and the averaged gel for each time point or condition was generated. Histograms for all the matched spots on all the gels, including the averaged gels, were then visually analyzed for reproducibility. All the spots showing reproducible changes on the histograms were then visually analyzed on the images of the gels to confirm the significance/reproducibility of the changes. Final confirmation was performed by calculating the fold change, which was set at a minimum of 1.5 except for spot 26 (1.4).

Image analysis of membranes subjected to immunoblotting and gels after autoradiography was carried using Adobe Photoshop Version 7.0. Different colors were applied to the total protein staining and to the phosphoprotein staining using Selective Color Tool, and different images of the same gel were then superimposed using the Opacity Tool. For image analyses involving radiolabeled proteins, multiple exposures of the gels were performed in order to reveal both the strongly labeled and the weakly labeled proteins.

2.8 Protein identification by LC-MS/MS

Protein spots that showed a $\geq$1.5-fold increase or reduction in intensity using either of the two staining methods were selected for further analyses, except for spot 26, which showed a lesser but reproducible 1.4-fold variation in the phosphoamino acid staining method. Spots chosen for sequencing were manually excised with a 1 mL pipet tip either from 7 Sypro Ruby stained gels or from 3 Coomassie stained gels and placed in a 96-well microtiter plate (Sigma, Milwaukee, WI, USA). The proteins were then automatically destained, reduced with DTT, alkylated with iodoacetamide, and digested with porcine trypsin (sequencing grade, Promega, Madison, WI, USA) using a MassPREP protein digest station (Micromass, Manchester, UK). The digest was evaporated to dryness, then dissolved in 12 μL of 0.1% aqueous TFA, of which 6 μL were analyzed by LC-MS/MS using a capLC ternary HPLC system (Waters, Milford, MA, USA) interfaced to a quadrupole-TOF (Q-TOF) Ultima Global hybrid tandem mass spectrometer fitted with a Z-spray nanoelectrospray ion source (Micromass). Solvents B and C comprised 0.2% formic acid in water, while solvent A consisted of 0.2% formic acid in ACN. The peptide digest sample was loaded onto a C18 trapping column (Symmetry 300, 0.35 × 5 mm Opti-pak; Waters) and washed for 3 min using solvent C at a flow rate of 30 μL/min. The flow path was then switched using a ten-port rotary valve, and the sample eluted onto a C18 analytical column (PepMap, 75 μm × 15 cm, 3-μm particle size; LC Packings). Separations were performed using a linear gradient of 0:100 to 60:40% A:B over 43 min. The composition was then changed to 80:20% A:B and held for 10 min to flush the column before re-equilibrating for 7 min at 0:100% A:B. Mass calibration of the Q-TOF instrument was performed using a product ion spectrum of Glu-fibrinopeptide B acquired over the m/z range of 50–1900. LC-MS/MS analysis was carried out using data-dependent acquisition, during which peptide precursor ions were detected by scanning from m/z 400 to 1900 in TOF MS mode. Multiply charged (2+, 3+, or 4+) ions rising above predetermined threshold intensity were automatically selected

for TOF MS/MS analysis, and product ion spectra acquired over the m/z range of 50–900. LC-MS/MS data were processed using ProteinLynx v2.15 software (Micromass) and searched against the NCBI nonredundant (nr) and EST_others database using MASCOT (Matrix Science Inc., Boston, MA, USA). Searches were performed using carbamidomethylation of cysteine as the fixed modification and oxidation of methionine as the variable modification, allowing for one missed cleavage during trypsin digestion.

2.9 RNA extraction, probe preparation, cDNA array hybridization, and data analysis

DNA microarrays were printed on UltraGAPS™ Slides (Corning Life Sciences, Acton, MA, USA) from 7741 ESTs corresponding to 6374 unigenes derived from a fertilized ovary cDNA libraries covering embryo development from zygote to late torpedo stages in *S. chacoense* [24]. This microarray was used to analyze gene expression profiles in ovaries 0 and 48 hours after pollination (HAP). Total RNA was extracted from unfertilized ovules (0 HAP) and from ovules 48 HAP using TRIzol® Reagent (Invitrogen, Burlington, ON, Canada) according to the manufacturer's instructions. RNA yield and purity were assessed by absorbance determination at both 260 and 280 nm. RNA was only used when the ratio Abs260 nm/Abs280 nm was higher than 1.7. RNA integrity was determined with the RNA 6000 Nano Assay Kit and the Agilent 2100 Bioanalyzer (Agilent Technologies, Mississavga, ON, Canada). Thirty micrograms of total RNA from 48 HAP ovaries were hybridized to microarrays along with the same amount of control RNA (0 HAP ovaries) for 16 h at 42°C. The experiment was carried out with four biological replicates that included two dye swaps. Labeling was performed with a cyanine 3-dCTP or cyanine 5-dCTP (1 mM; NEN Life Science, Boston, MA, USA, cat. no. NEL576 and 577). Hybridization and washing were performed as described in the CyScribe Post labeling Kit (GE Healthcare) in the CMTTM hybridization chamber (Corning). The DNA microarray slides were scanned with a ScanArray Lite scanner (Perkin Elmer-Cetus, Wellesley, CA, USA; Version 2.0) at 10-μm resolution. The resulting 16-bit TIFF files were quantified with QuantArray software (Perkin Elmer-Cetus; Versions 2.0 and 3.0). Normalization was performed with Lowess (Locally weighted scatter plot smoothing). Statistical analysis and visualization were performed with GeneSpring software (Silicon Genetics, Redwood City, CA, USA) using the available statistical tools (Student's *t*-test of replicate samples showing a variation different from 1).

3 Results and discussion

3.1 Comparison of phosphoprotein detection methods

The present study aimed at the identification of proteins and phosphoproteins differentially regulated during fertilization in plants. For this purpose, we have chosen a wild relative of the potato, *S. chacoense,* that is an obligate outcrosser due to the presence of a genetically determined reproductive barrier active in the style. The presence of this reproductive barrier, termed gametophytic self-incompatibility, involves rejection of pollen when both pistil and pollen share the same allele at the S locus, thus preventing the pollen tube from reaching the ovules and effecting fertilization [26]. This self-recognition and rejection system assures that only genetically different pollen can fertilize the flower, thus making selfing impossible. This, combined with manual pollinations, enables the synchronization of pollination, and thus, of fertilization over a limited time window.

Since the characterization of phosphoproteins still remains a difficult task [16] and no perfect method for their detection exists, three different detection methods were used and compared in order to ascertain the validity of the phosphoproteins detected. These included: (i) autoradiography after *in vivo* labeling with ^{32}P-orthophosphate, (ii) immunodetection using antibodies raised against phosphorylated residues, (iii) direct gel staining with a fluorophore specific for phosphoproteins. Since fertilization takes place from 36 h after pollination (HAP) in *S. chacoense,* and since pollination is known to induce some changes at a distance in the ovary before pollen tubes reach the ovaries [24, 27], 30 HAP ovaries were taken as controls and compared to 36, 42, and 48 h postpollination ovaries, where fertilization had taken place.

3.2 *In vivo* ^{32}P labeling

A 6 h period was determined as optimal to obtain a high level of radioactive labeling in the ovaries, and the analysis of proteins differentially phosphorylated after fertilization was carried out in two steps. Firstly, flowers were hand-pollinated in the greenhouse and after 24, 30, 36, or 42 h, inflorescence stems were cut and brought into a specially designed growth chamber to enable a safe *in vivo* labeling procedure (Fig. 1). Proteins were then isotopically labeled by feeding the cut inflorescence stems bearing 8–10 flowers with a small volume of ^{32}P-orthophosphate solution in a microtube for 20 min. The inflorescence stems were then placed in a conical flask containing water and left for 6 h. The proteins were extracted from the labeled ovaries and subjected to 2-DE. A total of 147 protein spots were detected on the autoradiogram, of which 90 protein spots (Fig. 2, right panel) could also be identified on the Sypro Ruby stained gel (Fig. 2, left panel). Numerous spots were also organized in the horizontal lines, suggesting different levels of phosphorylation of the same protein (Fig. 2, middle panel). Some of the phosphorylated proteins were present in such low amounts that they were under the detection threshold of the Sypro Ruby total protein stain (Fig. 2).

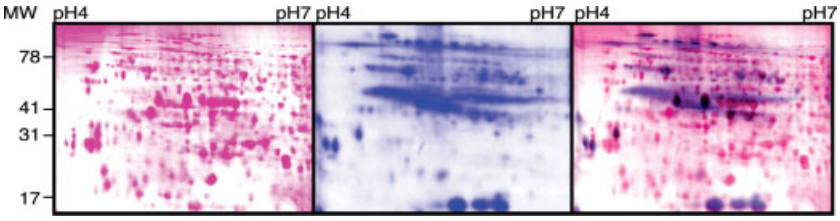

Figure 2. Comparison of the 2-DE patterns obtained from ^{32}P-labeling and Sypro Ruby (total protein) staining. One hundred micrograms of proteins extracted from ^{32}P *in vivo*-labeled ovaries harvested 48 HAP were separated on IEF strips pH 4–7 as first dimension and 10% acrylamide SDS gels as second dimension. The gel was then stained with Sypro Ruby (left panel, proteins colored in pink), then exposed to an autoradiography film and scanned (middle panel, proteins colored in blue). The superposition of the two images showing which proteins correspond to a phosphoprotein can be seen in the right panel (dual color).

3.3 Antibody detection

For antibody detection, flowers were hand-pollinated in the greenhouse and ovaries collected after 30, 36, 42, or 48 HAP. After 2-DE and electrotransfer of the protein on PVDF membranes, a different mix of mAb was used to detect phosphoserine (Fig. 3A), phosphothreonine (Fig. 3B), and phosphotyrosine (Fig. 3C) residues. Before antibody detection, Ponceau Red staining was used to visualize the total protein pattern. Merging of the two images in different colors enabled subsequent mapping of the proteins detected with the various antibodies (data not shown). A total of 155 spots could be detected with antiphosphoserine antibodies, while 284 spots were detected with antiphosphothreonine antibodies, and 222 spots were detected with antiphosphotyrosine antibodies (Table 1). Image analysis and overlapping of the patterns obtained with the different antibodies allowed identification of proteins that were simultaneously phosphorylated on different amino acids. All possible phosphorylation patterns were obtained with some proteins being phosphorylated on serine and threonine residues, serine and tyrosine residues, threonine and tyrosine residues, and some showing serine, threonine, and tyrosine phosphorylation (for example, spots #17, 26, 54 in Fig. 5). Although a greater number of protein spots had been identified by each individual antibody, only the ones that could be unambiguously assigned to a Ponceau Red stained protein were considered for the Venn diagram analysis shown in Fig. 3D. Figure 5 presents the complete compilation map of the phosphoprotein detection methods identified on a Sypro Ruby stained gel. Interestingly, even though putative phospho-isomers of some proteins can be observed on the membranes from for all three antibodies, the antiphosphotyrosine detection presented the most obvious phospho-isomer patterns with horizontal lines showing multiple phosphorylation states of the same protein for almost all proteins phosphorylated on tyrosine residues. Considering that each horizontal line of spots detected with antityrosine antibodies may be the same protein, the 222 identified spots would correspond to approximately 50 different proteins. This number is consistent with the fact that no tyrosine kinase similar to mammalian tyrosine kinases have been isolated in plants although some plant protein kinases have been shown to have dual kinase specificity, phosphorylating both Ser/Thr and Tyr residues [28, 29]. Furthermore, the characterization of a group of about 20 protein tyrosine phosphatases in *Arabidopsis* suggests a wider role of tyrosine phosphorylation in plants [30].

3.4 Phosphospecific protein dye

For phosphospecific protein dye detection, flowers were hand-pollinated in the greenhouse and ovaries collected after 30, 36, 42, or 48 HAP. After 2-DE, the gels were stained with the phosphospecific protein dye Pro-Q Diamond Phosphoprotein stain. Duration of the staining step had to be optimized and 47 min was chosen as the optimal time. With staining times longer than 47 min, the patterns obtained were very similar to those obtained from the total protein stain (Sypro Ruby), which suggests that a long staining period leads to a loss of staining specificity. Furthermore, even with this optimized staining time, more putative phosphoprotein spots were observed with Pro-Q Diamond Phosphoprotein stain than with either of other two methods. This, combined with the fact that general protein staining increases with the duration of staining, strongly suggests that this fluorophore is not absolutely specific for phosphoproteins. To test this, the staining pattern obtained with the Pro-Q Diamond stain was compared between ovary proteins extracted with added calyculine A (a phosphatase inhibitor) and a similar extract of ovary proteins treated with alkaline phosphatase for 1 h. The resulting gels are shown in Fig. 4. Although the staining of many spots was reduced after pretreatment with alkaline phosphatase (at least 67% of the spots could be counted as reduced or absent after alkaline phosphatase treatment), not all of them were affected. Because of the lack of absolute specificity of the phosphoprotein dye, only those spots that showed a decrease in intensity after alkaline phosphatase treatment were further considered and herein referred to as phosphoproteins detected by the Pro-Q Diamond Phosphoprotein stain method. Surprisingly, some of the spots showed increased staining after alkaline phosphatase treatment suggesting that, for some proteins, this treatment increased their stainability. The status of these latter as putative phosphoproteins is thus questionable.

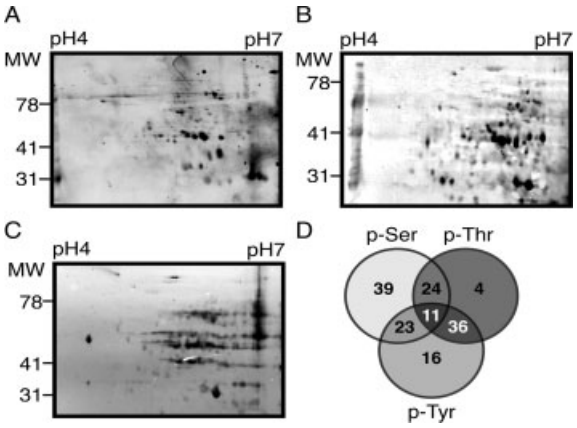

Figure 3. Comparison of the 2-DE patterns obtained with antiphospho-Ser, antiphospho-Thr, and antiphospho-Tyr antibody detection. (A) Detection of the phosphorylated proteins with antiphosphoserine antibody mix. (B) Detection of the phosphorylated proteins with antiphosphothreonine antibody mix. (C) Detection of the phosphorylated proteins with antiphosphotyrosine antibody mix. (D) Venn diagram analysis of the number of phosphoproteins crossdetected with different antibodies and matched on the Sypro Ruby gel.

3.5 Comparison of the three phosphoprotein detection methods

The phosphoproteins detected with these three detection methods were mapped onto a single gel to clearly visualize the degree of overlap obtained from the different methods (Fig. 5). Table 1 and Fig. 6 summarize the sensitivity of the three methods used (number of phosphoprotein spots detected) and the different levels of overlap observed. In total, with all phosphoprotein detection methods combined, 262 phosphorylated proteins could be mapped to the 619 proteins detected by Sypro Ruby staining, representing 42% of the total proteins. Among these 262 phosphoproteins, antibodies detected 184 proteins from which only 78 were also detected with either of other two methods (42%). Pro-Q Diamond phosphoprotein stain detected 111 proteins from which 76 were also detected with either of the other two methods (68%). The ^{32}P *in vivo* labeling method detected 90 spots from which 78 were also detected with either of other two methods (87%). Although the antibody detection method could be considered more sensitive from these results, it is also generally considered much less specific, especially for

Table 1. Comparison of different phosphoprotein detection methods. The total number of protein spots represents those detected using a general protein visualization method (Sypro Ruby or Ponceau Red) on the gel that was later subjected to a phosphoprotein detection method. The total number of phosphoproteins represents those detected using the given phosphoprotein detection method on the gel or membrane. The number of phosphoprotein spots detected on the Sypro Ruby-stained gel represent the number of phosphoprotein spots that could be mapped to a corresponding Sypro Ruby-stained spot (see Fig. 5)

Detection method used		Total number of protein spots detected	Total number of phospho-protein spots detected	Number of phosphoprotein spots detected on the Sypro Ruby-stained gel	Percentage of phospho-protein spots[a)]
Sypro Ruby staining		619	–	–	–
Ponceau/Antibody staining	Ponceau/antiP-Ser antibody	206	155	97	15.7
	Ponceau/antiP-Thr antibody	284	243	75	12.1
	Ponceau/antiP-Tyr antibody	357	222	86	13.9
	Proteins detected with at least 1 antibody	–	–	184	29.7
	Proteins detected with antiP-Ser + antiP-Tyr	–	–	23	3.7
	Proteins detected with antiP-Ser + antiP-Thr	–	–	24	3.9
	Proteins detected with antiP-Thr + antiP-Tyr	–	–	36	5.8
	Proteins detected with antiP-Ser + antiP-Tyr + antiP-Thr	–	–	11	1.8
	Detected only by antibody method	–	–	106	17.1
Sypro Ruby/^{32}P staining	All	453	147	90	14.5
	Detected only with ^{32}P	–	–	22	3.6
ProQ Diamond stain without/with phosphatase	All	353	236	111	17.9
	Detected only with ProQ Diamond method	–	–	34	5.5
Combination of different methods	Phosphoproteins detected by different methods	–	–	262	42.3
	Phosphoproteins detected with all three methods	–	–	23	3.7
	Proteins detected with ProQ Diamond + ^{32}P method	–	–	22	3.6
	Proteins detected with ProQ Diamond + antibody method	–	–	32	5.2
	Proteins detected with antibodies + ^{32}P	–	–	23	3.7

a) Determined from the total number of protein spots (619) detected from the Sypro Ruby gel.

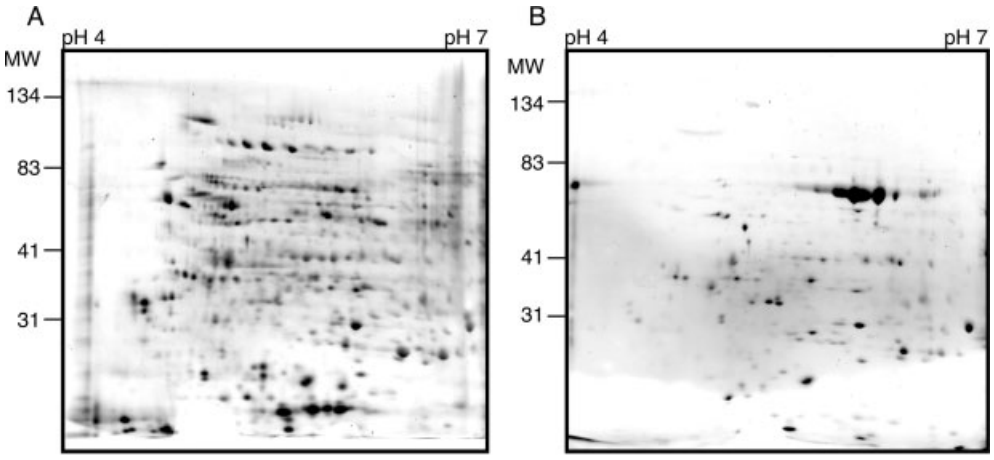

Figure 4. 2-DE patterns obtained with the Pro-Q Diamond phospho-specific stain before and after alkaline phosphatase treatment. (A) Pro-Q Diamond stained gel with proteins extracted from ovaries 0 h postpollination. (B) Pro-Q Diamond stained gel obtained after pretreatment of the ovary extracted proteins with alkaline phosphatase.

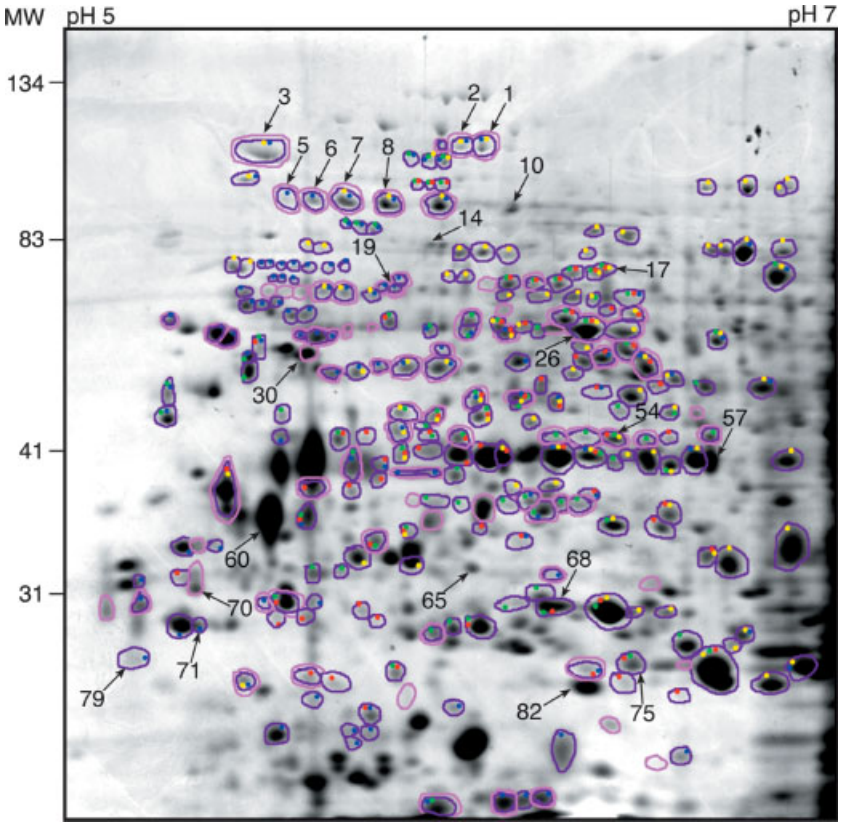

Figure 5. Compilation map of the phosphoproteins detected with the three different detection methods. Phosphoproteins detected by all the different methods were mapped onto a single gel made from proteins extracted from nonfertilized ovaries and stained with Sypro Ruby. Spots circled in pink represent phosphoproteins detected with the ^{32}P-orthophosphate *in vivo* labeling method. Spots circled in deep violet represent phosphoproteins detected from non *in vivo* labeling methods. Dots of different colors represent detection with Pro-Q Diamond (blue dot), antiphosphoserine antibody detection (yellow dot), antiphosphothreonine antibody detection (red dot), and antiphosphotyrosine antibody detection (green dot). For the Pro-Q Diamond detection method, only the proteins which had reduced staining after alkaline phosphatase treatment were considered to be phosphoproteins.

phosphoserine and phosphothreonine residues [31]. This is reflected in a much higher percentage of spots that could not be confirmed by any of the other two methods (58%). Detection with ^{32}P *in vivo* labeling was the more stringent method with the highest confirmation percentage, while ProQ Diamond staining gave an intermediate confidence level. However, even if the stringency of ^{32}P labeling method seems very appealing, this method can present some serious drawbacks when using it for comparative studies in tissues like flower branches. The length of absorption is very long, combined with the fact that ATP life is very short and that most of phosphorylation–dephosphorylation processes can happen

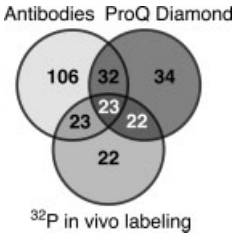

Figure 6. Venn diagram analysis of numbers of phosphoproteins detected with the three different detection methods used and matched on the Sypro Ruby gel.

very fast, it is almost impossible to track those instantaneous changes during fertilization with this method. Only 23 proteins were detected with all three methods simultaneously, representing 3.7% of the total proteins and 8.8% of all the phosphorylated proteins detected. These results clearly indicate that although there is no perfect method for phosphoprotein detection, and that some might be more appropriate depending on the tissue used, confirmation by alternative methods will significantly increase the assurance in assigning a protein as a phosphoprotein from a 2-DE gel analysis.

3.6 Analysis of proteins differentially expressed during fertilization

To identify proteins whose expression changes during fertilization, we analyzed 2-D gels containing proteins from ovaries 30, 36, 42, 48 HAP. Thirty HAP was taken as the control time point since fertilization has not yet taken place (pollen tubes have reached from two-thirds of the style to the base of the

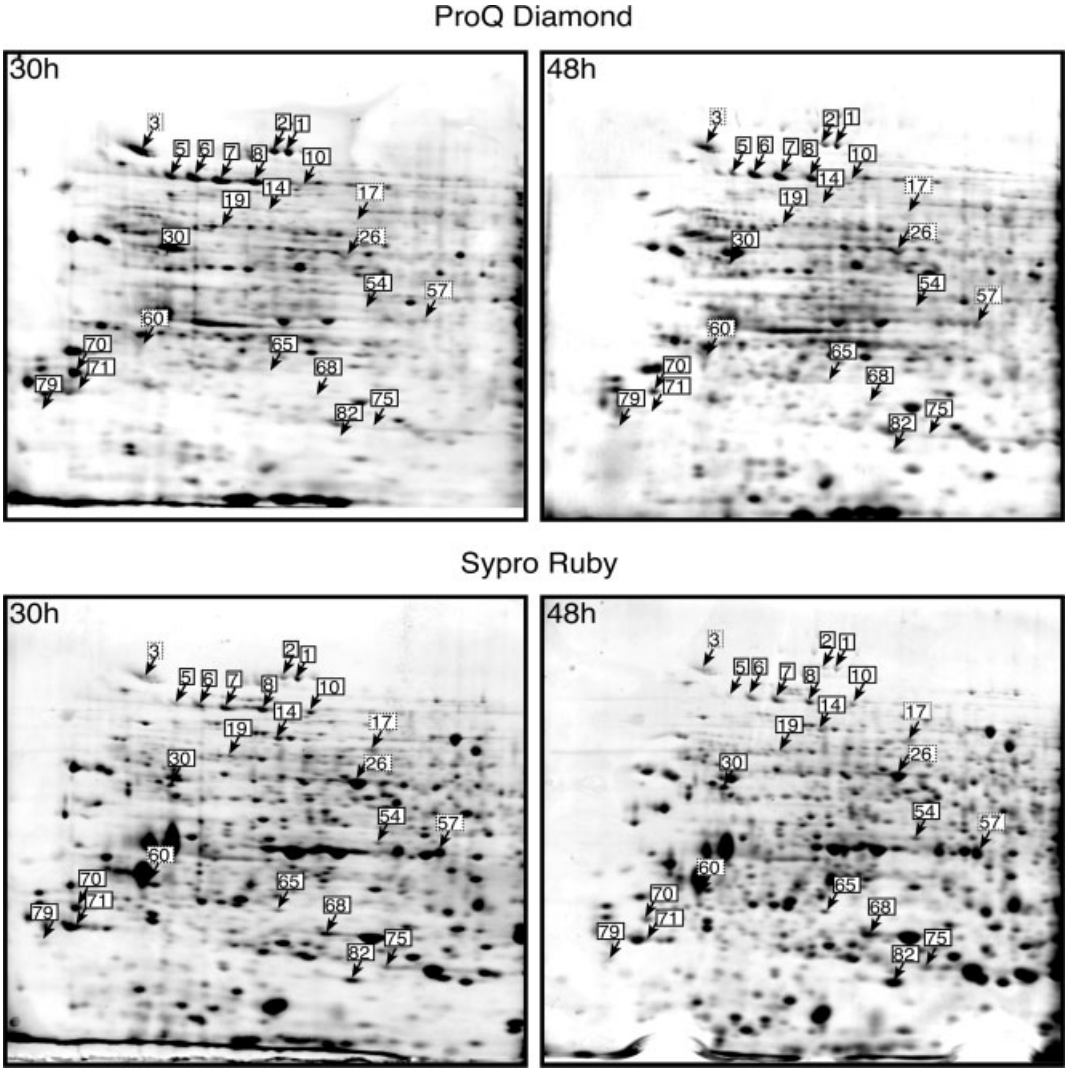

Figure 7. Time-course analysis of protein expression during fertilization as demonstrated by 2-DE. Upper panels: 2-DE gels stained with the phosphoprotein-specific dye. Lower panels: 2-DE gels stained with Sypro Ruby. Left: gels made from total protein extracted from ovaries 30 HAP (fertilization has not yet occurred). Right: gels made from total protein extracted from ovaries 48 HAP (fertilized ovaries). Arrows indicate proteins that showed a reproducible variation following fertilization and that were identified by LC-MS/MS. Dotted boxes indicate protein spots for which variations were only detected with the ProQ Diamond stain.

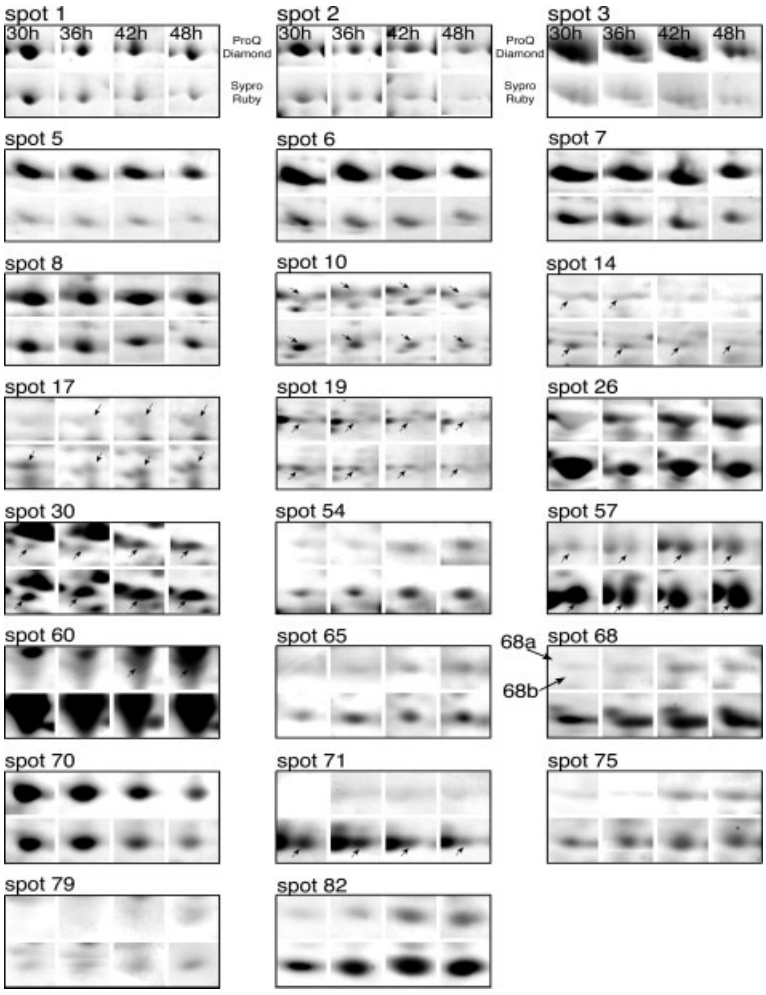

Figure 8. Time-course expression profiles of the proteins that were retained for MS/MS identification. Close-up view on the protein spots shown in Fig. 7 and that presented a reproducible change in staining with Sypro Ruby or Pro-Q Diamond. For each spot both the Pro-Q Diamond (top) and Sypro Ruby (bottom) gel portion is displayed before (30 HAP) and after the beginning of fertilization (36, 42, and 48 HAP). When multiple protein spots are present in the close-up view, an arrow indicates which spot is to be followed.

ovary) but account for pollination effects that can be observed at a distance in the ovary [24, 27]. Most of the ovules are fertilized between 36 to 42 HAP and the entire process is finished by 48 HAP. Different pH ranges of IPG strips were assayed (data not shown). Protein separation from p*I* 4 to 7 gave the best results, both in the total number of spots observed and in the overall quality and reproducibility of the 2-D gels, and so further analyses were performed using this pH range. Biological triplicates were produced for all time points and only proteins that showed reproducible changes in their expression profiles on all gels were considered. Figure 7 illustrates the gels at 30 and 48 HAP with the proteins that presented reproducible changes. The general pattern was very similar between all the different time points assayed, and overall only 38 proteins and phosphoproteins presented a reproducible change in their expression profiles as judged by the comparison of their normalized volumes. This was surprising as our previous study indicated that much more genes have a significant change in their expression as judged by their mRNA levels [24]. This can be explained in part by the discrepancies between changes in the abundance of specific mRNAs and their corresponding proteins, as this was previously reported [1–4]. It is also possible that the method used was not sensitive enough to detect some of those proteins, the limitations of 2-DE for separation of nonabundant and membrane proteins being well known. Within those proteins that showed a reproducible change only 24 had a fold change $\geq$1.4 and were chosen for further identification. A close-up view of these proteins can be seen in Fig. 8.

3.7 LC-MS/MS identification of the selected proteins

The chosen spots were digested *in situ* with trypsin and identified by LC-MS/MS. The sequence data was first searched against NCBI nr database using the MASCOT engine. Where identification failed, further searches were made against the EST_others database, and cDNA clones found in the EST_others database were then used to search for similarities by protein BLAST. This second search with the EST_others database enabled to greatly increase the identification of the protein spots, as only 11 spots out of 24 were identified in the first round, and 13 more in the second. This confirms once again the utility of EST resources in a

Table 2. List of proteins that present a reproducible change in staining with Pro-Q Diamond or Sypro Ruby identified by LC-MS/MS. Putative names of the identified proteins are listed with the theoretical and experimental MW in kDa and p*I*. Where appropriate, the phosphoprotein detection methods that detected the protein are indicated (Pro-Q stands for Pro-Q Diamond method with phosphatase treatment, ^{32}P for ^{32}P labeling, P-Ser for detection with antiphosphoserine antibody, P-Thr for antiphosphothreonine antibody and P-Tyr for antiphosphotyrosine antibody). Arrows indicate the variation in protein or phosphoprotein steady-state levels: (↑) up regulated, (↓) down regulated. The fold change was calculated with Image Master 2D Elite software.

Spot no.	GenBank accession number[a)]	Identity	Probability based MOWSE score	Peptides matched/ % coverage	Theoretical MW/p*I*[b)]	Experimental MW/p*I*	Phospho-detection	Fold change Sypro Ruby	Fold change Pro-Q Diamond[c)]	Fold change mRNA levels[d)]
1	gi|39822762 (gi|22329848)	Potato abiotic stress EST711862. This clone shares 49% identity with an unknown *A. thaliana* protein with a conserved DUF1296 region.	136	5/21	91/5.69	120/5.75	^{32}P, Pro-Q, P-Ser	↓3.6	↓1.7	na
2	gi|39831587 (gi|22329848)	Potato abiotic stress EST720687. This clone shares 45% identity with an unknown *A. thaliana* protein with a conserved DUF1296 region.	83	2/9	91/5.69	120/5.7	^{32}P, Pro-Q, P-Ser	↓5.3	↓2.7	na
3	gi|14643964 (gi|7267703)	Potato EST519098. This clone shares 60% identity with a putative *A. thaliana* DNA directed RNA polymerase with a conserved KH domain.	260	6/29	80/4.69	118/5.0	^{32}P, Pro-Q, P-Ser	↓3.6	↓3.1	na
5	gi|39814700 (gi|15225229)	Potato callus EST741357. This clone shares 64% identity with a nucleic acid binding protein with a conserved KH domain.	558	13/42	65/5.32	108/5.12	^{32}P, Pro-Q	↓3.0	↓1.9	na
6	gi|39814700 (gi|15225229)	Same EST as spot 5	553	16/54	65/5.32	108/5.25	^{32}P, Pro-Q	↓2.1	↓1.8	na
7	gi|39814700 (gi|15225229)	Same EST as spot 5	621	16/51	65/5.32	108/5.4	^{32}P, Pro-Q, P-Ser	↓1.9	↓1.4	na
8	gi|39814700 (gi|15225229)	Same EST as spot 5	648	17/51	65/5.32	108/5.75	^{32}P, Pro-Q, P-Ser	↓2.3	↓1.6	na
10	gi|39814700 (gi|15225229)	Same EST as spot 5	434	10/29	65/5.32	108/5.9	-	↓2.8	↓1.9	na
14	gi|7330642	Heat shock 68 kD protein, *S. tuberosum*.	653	18/22	73/6.37	83/5.82	P-Ser	↓2.4	↓2.2	↑1.2(97%)
17	gi|50934039	Putative succinate dehydrogenase flavoprotein α-subunit, *Oryza sativa*.	315	5/10	69.5/6.61	77/6.15	P-Ser, P-Thr, P-Tyr	1.0	↑7.2 48/42 HAP	↑1.4(80%)
19	gi|16221	Chaperonin heat shock 60 kD protein, *A. thaliana*.	371	11/21	62/5.66	72/5.5	^{32}P, Pro-Q	↓1.7	1.0	↑1.7(86%)
26	gi|19281	Enolase (cytosolic), tomato (*S. lycopersicum*).	1257	36/65	48/5.68	62/6.08	^{32}P, P-Ser, P-Thr, P-Tyr	↓ 1.3	↑1.4	↑1.5(94%)
30	gi|39830345 (gi|18398480)	Potato abiotic stress EST719445. This clone shares 76% identities with an unknown *A. thaliana* protein from the Arm/ β-catenin repeat family.	414	8/28	40/5.00	56/5.1	^{32}P	↑1.4	↑2.1	↑1.4(98%)

Table 2. Continued

Spot no.	GenBank accession number[a)]	Identity	Probability based MOWSE score	Peptides matched/ % coverage	Theoretical MW/p*I*[b)]	Experimental MW/p*I*	Phospho-detection	Fold change Sypro Ruby	Fold change Pro-Q Diamond[c)]	Fold change mRNA levels[d)]
54	gi|62891256 (gi|30684727)	Potato *in vitro* root EST 35087.2. This clone shares 76% identities with an *A. thaliana* aldose 1-epimerase protein.	257	7/31	37/5.88	41/6.25	^{32}P, P-Ser, P-Thr, P-Tyr	↑1.3	↑2.1	↓1.5(97%)
57	gi|10798652	Malate dehydrogenase (cytosolic), *Nicotiana tabacum*.	448	12/29	36/5.91	38/6.4	–	1.0	↑1.8	na
60	gi|14091665	Ran binding protein-1, *S. lycopersicum* (tomato).	233	11/38	25/4.88	33/4.95	–	1.0	↑1.8	↑1.6(97%)
65	gi|6058023 (gi|15242465)	Tomato mixed elicitor EST285608. This clone shares 77% identity with an *A. thaliana* chloroplast inorganic pyrophosphatase.	141	3/11	33/5.72	32/5.75	–	↑2.0	↑2.4 48/ 36HAP	↑1.2(89%)
68a	gi|24636598	Ascorbate peroxidase, *S. tuberosum*	295	8/30	27.4/5.43	31/6.0	P-Thr, P-Tyr	↑1.4	↑4.8 48/ 36HAP	↑1.2(95%)
68b	gi|559005	Ascorbate peroxidase, *N. tabacum*.	294	7/38	27.4/5.43	31/6.1	P-Thr, P-Tyr	↑1.4	↑4.8 48/ 36HAP	↑1.2(91%)
70	gi|17432522	ssDNA binding protein SEBF, *S. tuberosum*.	183	4/17	31/4.65	30/4.62	^{32}P, Pro-Q	↓2.4	↓2.4	↑1.2(98%)
71	gi|34907258	Putative NAC α-chain, *O. sativa*.	127	2/13	22/4.39	28/4.62	Pro-Q	↓1.7	–	↑1.4(85%)
75	gi|28192427	Dehydroascorbate reductase, *N. tabacum*.	107	3/14	24/7.7	27/6.18	P-Thr, P-Tyr	↑2.1	↑1.4	na
79	gi|13615355 (gi|7546725)	Potato EST495893. This clone shares 85% identity with the tomato MAF1 gene (MFP1 attachment factor 1).	213	4/28	16/4.34	26/4.4	Pro-Q	↑6.9	↑>10	↑1.3(98%)
82	gi|5899947 (gi|1743356)	Tomato mixed elicitor EST284057. This clone shares 89% identity with the proteasome delta subunit, *N. tabacum*.	332	9/37	25/5.18	26/6.06	–	↑1.4	↑3.5	↑1.5(98%)

na: Not available in our *S. chacoense* EST database and in our 7K *S. chacoense* array set.

N1: One of the identified peptides (LLTQDTFHEVK) is part of the DUF1296 region.

a) When the only match was the EST, the GenBank accession number given is of the EST clone and the GenBank accession number of protein to which this clone has the most similarity is given in parenthesis.

b) When the only match was the EST, the theoretical molecular weight and p*I* given were of the proteins to which this EST has the most identity.

c) Unless otherwise stated, the fold change value was determined between 48 and 30 HAP. When it was impossible to calculate a value for a time point due to faintness, the next one was chosen and indicated in the table.

d) As determined through cDNA microarray analysis (Statistical analysis using the ANOVA 1-Way Test with a Benjamini and Hochberg multiple testing correction algorithm with a p value ≤ 0.01). For this analysis, the EST from our database closest to the MS/MS match was analyzed and percentage sequence identity is shown in parenthesis.

proteomic study of any species for which a genome sequence is unavailable [32]. While the *S. chacoense* genome has not been sequenced, a vast collection of ESTs from the closely related species *Solanum lycopersicum* (tomato) and *Solanum tuberosum* (potato) are available as well as ESTs from a *S. chacoense* ovary-specific unigene set [24]. Table 2 shows the protein identifications and, when relevant, which phosphoprotein detection method also detected the protein. Out of 24 spots sequenced only five had not been detected by any phosphoprotein detection method. The fold change varia-

tions for both Sypro Ruby and ProQ Diamond stained gels (up- or down-regulated) are also shown in the Table 2. Three identified proteins are involved in protein synthesis and assembly: (i) the heat shock 68 kD protein (HSP 68, spot 14), (ii) the heat shock 60 kD chaperonin protein (HSP60, spot 19), and (iii) the putative nascent polypeptide associated complex (NAC) alpha chain (α-NAC) (spot 71). All the three proteins were down regulated in our study (Figs. 7 and 8). The HSPs that were identified are molecular chaperones. Their binding to polypeptides helps to fold and assemble them after their synthesis and also to prevent their stress-induced denaturation [33]. Both HSPs seem to be phosphorylated, however, HSP 68 was detected only with antiphospho-Ser antibody, while HSP 60 was detected with ^{32}P labeling and Pro-Q Diamond staining. α-NAC is a part of NAC composed of α and β chains. NAC can reversibly bind to eukaryotic ribosomes and is probably the first cytosolic protein to contact nascent polypeptide chains emerging from the ribosome [34]. It has been suggested that NAC is involved in protein sorting and translocation and that it can prevent mistargeting of nascent polypeptide chains to the ER [35]. Furthermore, several lines of evidence suggested that the α-NAC could function as a transcriptional coactivator [36, 37]. It was also proposed that in animals α-NAC is responsible of controlling FADD, a protein with an important role in apoptosis and other nonapoptotic events [38]. The function of plant NAC still remains largely unknown with the only report proposing that it is a target of salt toxicity [39]. In our study, we identified it as a phosphoprotein with two methods, ^{32}P labeling and Pro-Q Diamond staining.

Another three proteins that were identified may have a role in cytoskeleton and cell division: (i) a protein similar to armadillo (Arm)/β-catenin repeat family protein (spot 30), (ii) a protein similar to the Matrix attachment region binding Filament like Protein (MFP1) attachment factor 1 (MAF1, spot 79), and (iii) the Ran binding protein-1 (RanBP1, spot 60). All three proteins were up-regulated during fertilization (Fig. 7 and 8). Arm repeat proteins contain tandem copies of a degenerate protein sequence motif that forms a conserved 3-D structure. In animals, Arm/β-catenin proteins are implicated in cytoskeletal regulation, binding directly to the intracellular tail of cadherin through its Arm repeats [40]. The N-terminus of β-catenin in turn interacts with α-catenin [41] which interacts with actin [42]. In addition to their cytoskeletal functions, β-catenin and its homologues act as regulators of gene expression, both during development and throughout adult life [43, 44]. They are involved in signaling by the Wnt growth factor recruiting the basal transcription machinery to promoter regions of Wnt target genes [45]. Interestingly, this protein (spot 30) is phosphorylated in plants as detected by the ^{32}P *in vivo* labeling method. Spot 79, highly similar to the MAF1 protein from tomato, is a small serine/threonine rich protein interacting with MFP1. It was detected as a phosphoprotein by the Pro-Q Diamond method. MFP1 and MAF1 are components of nuclear substructure that connects the nuclear envelope and the internal nuclear matrix. Interestingly, the tomato MAF1 gene is more strongly expressed in young fruits and flowers [46]. Spot 60, the Ran binding protein 1 (RanBP1) is a protein binding to Ran (Ras-related nuclear small GTP-binding protein). Together with Ran-GTPase-activating protein, it promotes the hydrolysis of GTP on Ran. In *Arabidopsis thaliana*, At-RanBP1c is critically involved in root growth and development. The promotion of GTP hydrolysis by the Ran/RanGAP/AtRanBP1c complex in the cytoplasm, and the resulting concentration gradient of Ran-GDP to Ran-GTP across the nuclear membrane, could be important in the regulation of auxin-induced mitotic progression in root tips of *A. thaliana* [47, 48]. Overexpression of RanBP1 in mammalian cells induces multipolar spindles through loss of cohesion in mitotic centrosomes. Specifically, RanBP1 excess induces splitting of mother and daughter centrioles at spindle poles; the resulting split centrioles can individually organize functional microtubule arrays, giving rise to functional spindle poles [49]. It is thought that during double fertilization in plants, sperm cells are transported in the embryo sac by a cytoskeletal system [50]. The up-regulation of the proteins related to cytoskeleton in our study would agree with this hypothesis.

Among the other identified proteins, five can be considered as housekeeping enzymes, involved in respiration, citric acid cycle, glycolysis, and energy metabolism: (i) a cytosolic enolase (spot 26), (ii) a putative succinate dehydrogenase flavoprotein alpha subunit (spot 17), (iii) a protein similar to aldose 1-epimerase family protein (spot 54), (iv) a cytosolic malate dehydrogenase (spot 57), and (v) a chloroplastic inorganic pyrophosphatase (spot 65). During fertilization and early embryogenesis, metabolism becomes highly active as the ovary requires extra energy supplies to start the transformation of the mostly quiescent egg cell (oocyte) into a complex embryo. Enolase, succinate dehydrogenase flavoprotein alpha subunit, aldose 1-epimerase family protein, malate dehydrogenase, and inorganic pyrophosphatase may be important for activation of the entire energy-producing pathway [39, 51, 52]. Enolase seems to be slightly down regulated as judged from the Sypro Ruby stained gels, but the Pro-Q Diamond staining clearly increases (Figs. 7 and 8). Since we can confirm its phosphorylation state with other methods (Fig. 5 and Table 2), the increased staining with ProQ Diamond in this case suggests an increase in total phosphorylation of the protein. Enolase was shown to accumulate during mammalian embryogenesis [53] as well as during somatic embryogenesis in *Picea glauca* [32]. In our timeframe, which precedes embryogenesis, a slight decrease in the amount of enolase is observed while it is becoming more phosphorylated. It is possible that phosphorylation activates it during fertilization. We show that it is phosphorylated on serine, threonine, and tyrosine residues (Fig. 5 and Table 2). Detection of enolase isoforms with different p*I* values and suggesting posttranslation modifications has been shown in rice seedling [54]. Furthermore, a maize eno-

lase has also been shown to be the substrate of a 57 kD dual-specific protein kinase, being mainly phosphorylated on serine and tyrosine residues [55], thus confirming our identification of enolase as a phosphoprotein. The levels of expression of the putative succinate dehydrogenase flavoprotein alpha subunit does not change as judged from total staining, while its phosphorylation state increases as judged with ProQ Diamond staining (Figs. 7 and 8). We also confirmed its phosphorylation state by antibodies, and it seems to be phosphorylated on serine, threonine, and tyrosine residues. The last two enzymes are up regulated (Figs. 7 and 8). The aldose 1-epimerase family protein (spot 54) is detected as a phosphoprotein through both ^{32}P *in vivo* labeling and antibody detection, being phosphorylated on serine, threonine, and tyrosine residues (Fig. 5 and Table 2). Biosynthetic pathways that involve a release of pyrophosphate (PPi) are driven to completion by inorganic PPase-mediated PPi hydrolysis. Since many important biosynthetic pathways, including purines, pyrimidines, and starch synthesis are localized in plastids, and contain reactions that generate PPi, chloroplastic inorganic pyrophosphatase may also be of importance in very active tissues like ovaries to drive these reactions in the direction of synthesis, and in eliminating PPi from the chloroplastic compartment [56]. In our study, we show that its protein level increases during fertilization (spot 65, Figs. 7 and 8).

Two of the identified proteins are involved in oxidative stress: ascorbate peroxidase (spot 68a and b) and dehydroascorbate reductase (spot 75). Ascorbate peroxidase was identified in two spots, maybe representing two different isoforms. Both, ascorbate peroxidase and dehydroascorbate reductase are involved in scavenging of reactive oxygen species (ROS). Those two enzymes are up regulated in our study (Figs. 7 and 8). One possible explanation is that they are produced in response of oxidative burst producing ROS in the degenerated synergids cells after sperm cell penetration or a global increase in metabolism and serve to protect the delicate ovule from those toxic ROS. Alternatively, ROS have recently been recognized as second messengers for diverse processes like pathogen defense responses, abiotic stress signaling, and polarized cell expansion [57, 58]. Both enzymes were detected as phosphoproteins with the antibody detection method and would be phosphorylated on threonine and tyrosine residues.

The expression of a protein corresponding to the proteasome delta subunit was increased during fertilization (spot 82, Figs. 7 and 8). It is known that proteasome activity is closely aligned with cell proliferation processes [32], and its increase could be explained by the increase in total protein synthesis observed immediately following fertilization and the beginning of embryogenesis. It was shown that during later stages of somatic embryo development in *P. glauca,* some proteasome subunits are down regulated, which the authors explain by the arrest of the proliferation state and the beginning of the differentiation state in the developing embryo [32]. In our study, the increase observed could correspond to the early proliferation state observed in the embryo, and in particular in the endosperm which starts to divide earlier than the zygote.

Finally, four proteins possibly involved in transcriptional regulation were identified. One of them, identified by two spots (spots 1 and 2) is similar to an unknown protein with a conserved DUF1296 region. Analysis of this protein reveals that it bears a C terminal region rich in glutamine, a common feature of transcriptional activators. The two spots most probably correspond to different phosphorylation states of the same protein. The phosphorylation state of this protein was confirmed by all the three methods. The antibody detection method suggests that it would be phosphorylated on serine residues and the protein abundance is down regulated during fertilization (Figs. 7 and 8). Two other proteins have a KH domain, which was proposed to be involved in nucleic acid binding [59]. The first one (spot 3) is similar to a putative DNA directed RNA polymerase, and its phosphorylation state was confirmed by all the three methods. It also seems to be phosphorylated on serine residues and is down regulated during fertilization (Figs. 7 and 8). The second one is an unknown protein with a KH domain and a C terminal rich in glutamine, suggesting that it may act as a transcription factor. It was identified in five different spots (spots 5, 6, 7, 8, 10) suggesting that they correspond to different phosphorylation states of the same protein. Phosphorylation status was confirmed by ^{32}P *in vivo* labeling and both Pro-Q Diamond and Sypro Ruby staining decrease after fertilization. The last protein (spot 70) corresponded to the silencing element binding factor (SEBF) transcriptional repressor, previously shown to negatively regulate the expression of the pathogenesis-related PR-10a gene in potato [60]. SEBF is homologous with chloroplast RNA binding proteins that possess consensus sequence-type RNA binding domains characteristic of heterogenous nuclear ribonucleoproteins (hnRNPs). This transcriptional regulator has been shown to bind the coding strand of the PR-10a silencing element in a sequence-specific manner. Furthermore, SEBF has been shown experimentally to be the substrate of a purified kinase activity in an *in vitro* phosphorylation assay from potato tuber extracts (Brisson, N., personal communication). In our study, phosphorylation status of spot 70 was confirmed by ^{32}P *in vivo* labeling and Pro-Q Diamond staining and both Pro-Q Diamond and Sypro Ruby staining decrease after fertilization, suggesting that derepression of SEBF target genes might occur rapidly following fertilization. Although only currently described as a transcription factor involved in defense responses in plants, the SEBF binding site was also found in numerous wound- or stress-inducible genes [60]. A wider role is suggested by the fact that SEBF expression has been detected in ovaries [24]. Furthermore, comparison of the SEBF binding site (PyTGTCNC) with other regulatory elements revealed a strong similarity to the auxin response element (AuxRE; TGTCTC) present in composite AuxRE. Since auxins regulate numerous aspects of plant growth and development,

including morphogenesis, cell elongation and cell division, this might suggest that this transcriptional repressor indeed has a wider role in plants.

3.8 Proteome and transcriptome comparison

Other studies have shown that the transcriptional reprogramming during the reproductive development leads to a significant enrichment of genes encoding proteins involved in metabolism, transcription, and cellular organization [24, 61]. Our study provides additional support for these findings as we show here that the steady-state levels of the proteins involved in those processes are modulated during fertilization. But, as already mentioned in the introduction section, numerous studies have pinpointed the discrepancies between the transcriptional and translational regulation levels. In order to assess this, we have used cDNA microarrays produced from 7741 ESTs corresponding to 6374 unigenes derived from a fertilized ovary cDNA librairies covering embryo development from zygote to late torpedo stages in *S. chacoense* [24]. Among the 18 different proteins obtained from the 24 protein spots sequenced, 14 had highly significant matches in our EST database. The nucleotide sequence percentage identity as well as their fold change is indicated in Table 2. As observed in other studies, there is no clear correlation between variations in mRNA and protein levels. In only half the cases did the mRNA variation observed in line with the protein fold change observed. Furthermore, the mRNA variations observed were very weak, again emphasizing the importance of conducting proteomic analyses to provide critical information on the amount and/or activity of proteins at a given time in a given tissue, or in response to a given stimulus or treatment.

4 Concluding remarks

In this study, we reported a comparative proteomic analysis of the *S. chacoense* ovary proteins during fertilization. Eighteen different proteins involved in fertilization were identified. Some appear directly implicated in the fertilization process (cytoskeletal proteins), some in the preparation for embryogenesis (*e.g.,* proteins from oxidative stress, housekeeping category), while the role of others remains unknown (α-NAC, several new putative transcription factors). This is the first proteomic study of changes during plant fertilization, and it provides a starting point for further investigation into functions of proteins involved in fertilization. Deeper proteomic analysis will help us better understand the fertilization mechanism in plants. For example, it would be important to identify the membrane proteins, which are believed to play key roles in signal transduction in order to understand the signal transduction during fertilization in plant.

Three different methods for phosphoprotein detection were also compared for their sensitivity and efficiency. We show that, as expected, *in vivo* labeling with ^{32}P is the most stringent method to detect the phosphoproteins, as it shows the highest rate of confirmation with other methods, compared to immunodetection which seemed to identify many more phosphorylated proteins but has a lower rate of confirmation by other methods. ProQ Diamond method could be placed between the two for its specificity; however, the specificity of this method was greatly increased by the phosphatase test. We show that the overlap between the three methods is very small, indicating that no one method alone is good enough to be relied upon and that a thorough evaluation of the needs of the experiment (comparative or qualitative study) along with the combination of different methods should be used for phosphoprotein detection during proteomic studies.

We thank Martin O'Brien for his help during the in vivo labeling and Gabriel Téodorescu for greenhouse plant care and maintenance. This work was supported by the Natural Sciences and Engineering Research Council of Canada (NSERC) and the Canada Research Chair program. Funding for proteomics infrastructure at PBI was provided by the Saskatchewan provincial government and the National Research Council of Canada (NRCC). K. Vyetrogon is the recipient of an M. Sc. fellowship from Le Fonds Québécois de la Recherche sur la Nature et les Technologies (FQRNT, Québec). D. P. Matton holds a Canada Research Chair in Functional Genomics and Plant Signal Transduction.

5 References

[1] Anderson, L., Seilhamer, J., *Electrophoresis* 1997, *18*, 533–537.

[2] Anderson, N. L., Anderson, N. G., *Electrophoresis* 1998, *19*, 1853–1861.

[3] Gygi, S. P., Rist, B., Gerber, S. A., Turecek, F. *et al.*, *Nat. Biotechnol.* 1999, *17*, 994–999.

[4] Ideker, T., Galitski, T., Hood, L., *Annu. Rev. Genomics Hum. Genet.* 2001, *2*, 343–372.

[5] Zivy, M., Vienne, D., *Plant Mol. Biol.* 2000, *44*, 575–580.

[6] Bove, J., Jullien, M., Grappin, P., *Genome Biol.* 2002, *3*, reviews 1002.1–1002.5.

[7] Weterings, K., Russell, S. D., *Plant Cell* 2004, *16*, S107–S118.

[8] Finnie, C., Melchior, S., Roepstorff, P., Svensson, B., *Plant Physiol.* 2002, *129*, 1308–1319.

[9] Gallardo, K., Job, C., Groot, S. P., Puype, M. *et al.*, *Plant Physiol.* 2002, *129*, 823–837.

[10] Gallardo, K., Le Signor, C., Vandekerckhove, J., Thompson, R. D., Burstin, J., *Plant Physiol.* 2003, *133*, 664–682.

[11] Hajduch, M., Ganapathy, A., Stein, J. W., Thelen, J. J., *Plant Physiol.* 2005, *137*, 1397–1419.

[12] Ostergaard, O., Finnie, C., Laugesen, S., Roepstorff, P., Svennson, B., *Proteomics* 2004, *4*, 2437–2447.

[13] Sheoran, I. S., Olson, D. J., Ross, A. R., Sawhney, V. K., *Proteomics* 2005, *5*, 3752–3764.

[14] Vensel, W. H., Tanaka, C. K., Cai, N., Wong, J. H. *et al.*, *Proteomics* 2005, *5*, 1594–1611.

[15] Okamoto, T., Higuchi, K., Shinkawa, T., Isobe, T. *et al.*, *Plant Cell Physiol.* 2004, *45*, 1406–1412.

[16] Laugesen, S., Bergoin, A., Rossignol, M., *Plant Physiol. Biochem.* 2004, *42*, 929–936.

[17] Venter, J. C., Adams, M. D., Myers, E. W., Li, P. W. *et al.*, *Science* 2001, *291*, 1304–1351.

[18] Zolnierowicz, S., Bollen, M., *EMBO J.* 2000, *19*, 483–488.

[19] Initiative, T. A. G., *Nature* 2000, *408*, 796–815.

[20] Kerk, D., Bulgrien, J., Smith, D. W., Barsam, B. *et al.*, *Plant Physiol.* 2002, *129*, 908–925.

[21] Schulenberg, B., Aggeler, R., Beechem, J. M., Capaldi, R. A., Patton, W. F., *J. Biol. Chem.* 2003, *278*, 27251–27255.

[22] Schulenberg, B., Goodman, T. N., Aggeler, R., Capaldi, R. A., Patton, W. F., *Electrophoresis* 2004, *25*, 2526–2532.

[23] Steinberg, T. H., Agnew, B. J., Gee, K. R., Leung, W. Y. *et al.*, *Proteomics* 2003, *3*, 1128–1144.

[24] Germain, H., Rudd, S., Zotti, C., Caron, S. *et al.*, *Plant Mol. Biol.* 2005, *59*, 515–532.

[25] Bradford, M. M., *Anal. Biochem.* 1976, *72*, 248–254.

[26] de Nettancourt, D., *Sex. Plant Reprod.* 1997, *10*, 185–199.

[27] Lantin, S., O'Brien, M., Matton, D. P., *Plant Mol. Biol.* 1999, *41*, 371–386.

[28] Rudrabhatla, P., Rajasekharan, R., *Biochemistry* 2004, *43*, 12123–12132.

[29] Rudrabhatla, P., Reddy, M. M., Rajasekharan, R., *Plant Mol. Biol.* 2006, *60*, 293–319.

[30] Luan, S., *Proc. Natl. Acad. Sci. USA* 2002, *99*, 11567–11569.

[31] Raggiaschi, R., Gotta, S., Terstappen, G. C., *Biosci. Rep.* 2005, *25*, 33–44.

[32] Lippert, D., Zhuang, J., Ralph, S., Ellis, D. E. *et al.*, *Proteomics* 2005, *5*, 461–473.

[33] Gimenez-Abian, M. I., Rozalen, A. E., Carballo, J. A., Botella, L. M. *et al.*, *Protoplasma* 2004, *223*, 191–196.

[34] Beatrix, B., Sakai, H., Wiedmann, M., *J. Biol. Chem.* 2000, *275*, 37838–37845.

[35] Rospert, S., Dubaquie, Y., Gautschi, M., *Cell Mol. Life Sci.* 2002, *59*, 1632–1639.

[36] Moreau, A., Yotov, W. V., Glorieux, F. H., St-Arnaud, R., *Mol. Cell Biol.* 1998, *18*, 1312–1321.

[37] Yotov, W. V., Moreau, A., St-Arnaud, R., *Mol. Cell Biol.* 1998, *18*, 1303–1311.

[38] Stilo, R., Liguoro, D., di Jeso, B., Leonardi, A., Vito, P., *Biochem. Biophys. Res. Commun.* 2003, *303*, 1034–1041.

[39] Yan, S., Tang, Z., Su, W., Sun, W., *Proteomics* 2005, *5*, 235–244.

[40] Aberle, H., Butz, S., Stappert, J., Weissig, H. *et al.*, *J. Cell Sci.* 1994, *107*, 3655–3663.

[41] Aberle, H., Schwartz, H., Hoschuetzky, H., Kemler, R., *J. Biol. Chem.* 1996, *271*, 1520–1526.

[42] Rimm, D. L., Koslov, E. R., Kebriaei, P., Cianci, C. D., Morrow, J. S., *Proc. Natl. Acad. Sci. USA* 1995, *92*, 8813–8817.

[43] Coates, J. C., *Trends Cell Biol.* 2003, *13*, 463–471.

[44] Stadeli, R., Hoffmans, R., Basler, K., *Curr. Biol.* 2006, *16*, R378–R385.

[45] Hecht, A., Litterst, C. M., Huber, O., Kemler, R., *J. Biol. Chem.* 1999, *274*, 18017–18025.

[46] Gindullis, F., Peffer, N. J., Meier, I., *Plant Cell* 1999, *11*, 1755–1768.

[47] Kim, S. H., Arnold, D., Lloyd, A., Roux, S. J., *Plant Cell* 2001, *13*, 2619–2630.

[48] Kim, S. H., Roux, S. J., *Planta* 2003, *216*, 1047–1052.

[49] Di Fiore, B., Ciciarello, M., Mangiacasale, R., Palena, A. *et al.*, *J. Cell Sci.* 2003, *116*, 3399–3411.

[50] Cheung, A. Y., Wu, H., Di Stilio, V., Glaven, R. *et al.*, *Ann. Bot.* 2000, *85*, 29–37.

[51] Cooley, J. W., Vermaas, W. F., *J. Bacteriol.* 2001, *183*, 4251–4258.

[52] Timson, D. J., Reece, R. J., *FEBS Lett.* 2003, *543*, 21–24.

[53] Barbieri, G., De Angelis, L., Feo, S., Cossu, G., Giallongo, A., *Differentiation* 1990, *45*, 179–184.

[54] Tanaka, N., Mitsui, S., Nobori, H., Yanagi, K., Komatsu, S., *Mol. Cell. Proteomics* 2005, *4*, 796–808.

[55] Trojanek, J. B., Klimecka, M. M., Fraser, A., Dobrowolska, G., Muszynska, G., *Acta Biochim. Pol.* 2004, *51*, 635–647.

[56] Schulze, S., Mant, A., Kossmann, J., Lloyd, J. R., *FEBS Lett.* 2004, *565*, 101–105.

[57] Carol, R. J., Takeda, S., Linstead, P., Durrant, M. C. *et al.*, *Nature* 2005, *438*, 1013–1016.

[58] Uhrig, J. F., Hulskamp, M., *Curr. Biol.* 2006, *16*, R211–R213.

[59] Nagai, K., *Curr. Opin. Struct. Biol.* 1996, *6*, 53–61.

[60] Boyle, B., Brisson, N., *Plant Cell* 2001, *13*, 2525–2537.

[61] Hennig, L., Gruissem, W., Grossniklaus, U., Kohler, C., *Plant Physiol.* 2004, *135*, 1765–1775.

